The Astrophysical Journal, 936:52 (7pp), 2022 September 1 https://doi.org/10.3847/1538-4357/ac85bd

Mechanism for the Efficient Homogeneous Nucleation of Ice in a Weakly Ionized, Ultracold Plasma

Paul M. Bellan
Applied Physics and Materials Science, California Institute of Technology, 1200 E. California Blvd., Pasadena, CA 91125, USA; pbellan@caltech.edu
Received 2022 April 29; revised 2022 July 29; accepted 2022 July 30; published 2022 August 30

Abstract

It is proposed that the rapid observed homogeneous nucleation of ice dust in a cold, weakly ionized plasma depends on the formation of hydroxide (OH^-) by fast electrons impacting water molecules. These OH^- ions attract neutral water molecules because of the high dipole moment of the water molecules and so hydrates of the form $(OH)^-(H_2O)_n$ are formed. The hydrates continuously grow in the cold environment to become macroscopic ice grains. These ice grains are negatively charged as a result of electron impact and so continue to attract water molecules. Because hydroxide is a negative ion, unlike positive ions, it does not suffer recombination loss from collision with plasma electrons. Recombination with positive ions is minimal because positive ions are few in number (weak ionization) and slow-moving as result of being in thermal equilibrium with the cold background gas.

Unified Astronomy Thesaurus concepts: Circumstellar dust (236); Ice formation (2092); Plasma physics (2089); Water vapor (1791); Accretion (14); Dielectronic recombination (2061); Photoelectron spectroscopy (2097); Hydroxyl sources (772); Circumstellar grains (239); Interstellar dust (836); Silicate grains (1456); Interstellar dust processes (838)

1. Introduction

Grains of water ice occur in many terrestrial and extraterrestrial contexts. Examples include noctilucent clouds (Vaste 1993), comet tails (Protopapa et al. 2014), Saturn's diffuse rings (Vahidinia et al. 2011), plumes ejected by Enceladus (Dong et al. 2015), protoplanetary disks (Terada et al. 2007), and matter orbiting black holes (Moultaka et al. 2015). In order for these grains to nucleate, there must be preexisting water vapor or preexisting hydrogen and oxygen that could make water. Mechanisms for ice nucleation are categorized as being either heterogeneous or homogeneous: Heterogeneous nucleation involves ice forming as a cover or mantle on a preexisting non-ice solid material such as silicate or carbon whereas homogeneous nucleation is the situation where ice forms with no non-ice substrate. Studies of tropospheric (lower atmosphere) ice formation have shown that heterogeneous nucleation dominates homogeneous nucleation by orders of magnitude (Pruppacher & Klett 2010). This tropospheric domination of heterogeneous nucleation has generally been presumed to extend to noctilucent clouds (mesosphere) (Gumbel & Megner 2009) and to extraterrestrial contexts (Seki & Hasegawa 1983; Jones & Williams 1984). However, these nontropospheric contexts differ by being ultracold (gas temperature 150 K or less) and weakly ionized.

The paradigm that homogeneous nucleation is negligible compared to heterogeneous nucleation requires the preexistence of non-ice solid material. It is generally presumed that this solid material is silicate (Seki & Hasegawa 1983) in the context of protoplanetary disks. For noctilucent clouds, it is generally presumed that the solid material is carbon smoke from ablating micrometeoroids (Gumbel & Megner 2009); this solid material is called meteor smoke particle (MSP). However, various observations cast doubt on this paradigm:

1. The presumption that extraterrestrial water ice can exist only as a coating on silicate cores is clearly invalid for Saturn's rings where in situ mass spectrometry of ring ice grains by the Cassini spacecraft's Cosmic Dust Analyzer (CDA) showed that dust grains were composed of either water ice or silicate (Hsu et al. 2018), but not of both.
2. The spectra of Saturn's rings show water ice but no evidence of silicates (Spilker et al. 2003).
3. Potapov et al. (2021) showed that fits to certain protoplanetary disk infrared absorption spectra were best explained using pure water ice rather than a combination of ice and silicates.
4. There is minimal observational evidence for the existence of MSPs at the location where noctilucent clouds form, and there is minimal evidence that micrometeoroids deposit MSPs (Rapp & Thomas 2006; Hedin et al. 2014).
5. Murray & Jensen (2010) and Zasetsky et al. (2009) have postulated that homogeneous nucleation can occur in noctilucent clouds. An important feature of the Murray/Jensen and Zasetsky at al. papers is the realization that at the very low temperatures and pressures of interest, nucleation likely occurs in a quite different manner from nucleation in the tropospheric terrestrial atmosphere.
6. An ice dusty plasma experiment by Shimizu et al. (2010) at the Max Planck Institute for Extraterrestrial Physics showed that water-ice grains would spontaneously nucleate in a weakly ionized plasma formed from a mixture of D_2 and O_2 if the electrodes were cooled by liquid nitrogen so that the background gas would be at a low temperature. Shimuzu et al. modeled their experiment assuming that the nucleation was heterogeneous (ice nucleated about non-ice seed particles) but noted that there was no experimental evidence for the existence of the assumed seed particles.

Table 1
Similarity between Three Different Situations where Ice Grains Form in a Weakly Ionized Plasma Having a Cold Background Gas

	Laboratory Experiment	Mesosphere	Protoplanetary Disk, Midplane
Gas temperature	190 K	140 K	10–100 K
Gas density	5×10^{21} m^{-3}	5×10^{20} m^{-3}	10^{18}–10^{20} m^{-3}
Gas pressure	10 Pa	1 Pa	0.001–0.1 Pa
Ionization fraction	10^{-6}	10^{-12}	10^{-10}–10^{-6}

Notes. Lab experiment from Chai & Bellan (2013) and Marshall et al. (2017), mesophere density from Table 5 of Rapp et al. (2001), and protoplanetary disk from Figures 7, 9, 10, and 12 in Woitke et al. (2009).

7. An ice dusty plasma experiment at Caltech (Chai & Bellan 2013, 2015a, 2015b; Marshall et al. 2017) has shown that ice spontaneously nucleates when a small amount of water vapor is injected into a weakly ionized plasma if the plasma background gas is cold (<200 K) and above a critical pressure. Once nucleation has occurred, the pressure can be lowered, at which point the ice grains grow quickly to a large size within 10–100 s. The ice grains are long, slightly dendritic spindles that are highly charged. The system behaves as a classic dusty plasma with the additional feature that the spindles self-align so as to be mutually parallel. The experimental parameters are similar to the presumed parameters of protoplanetary disks and noctilucent clouds. Specifically, the background gas density of the lab experiment is within one or two orders of magnitude of these naturally occurring situations, the background gas temperature is similarly cold, the degree of ionization is similarly small, and water molecules are similarly present. These similarities are shown in Table 1. Because protoplanetary disk parameters vary considerably depending on the distance from the star and the altitude above the midplane, it is quite plausible that the lab experiment exactly duplicates some specific localized protoplanetary disk region.

2. Classic Nucleation Theory Summarized

Gas-phase ice nucleation is conventionally assumed to occur in accordance with classic nucleation theory (CNT), which postulates that nucleation is heterogeneous and results from the interplay between the thermodynamic concepts of Gibbs free energy and surface tension. CNT was originally formulated for liquid drops but has been proposed to extrapolate to ice nucleation. CNT assumes that a newborn liquid drop (in the ice extrapolation, newborn ice grain) is spherical and has a radius r that relates to the surface tension. This model was reviewed by Rapp & Thomas (2006) and by Gumbel & Megner (2009) in the context of noctilucent cloud ice grains and the process was that of water nucleating on charged MSPs. A critical assumption in CNT is that nucleation can be described using bulk matter properties. CNT shows using considerations of surface tension that there is an energy barrier preventing nucleation at small radius; this is because the force associated with surface tension is inversely proportional to the radius of curvature of the surface so this force becomes infinite as the radius approaches zero.

Gumbel and Megner noted that ionic nucleation could be an alternate to MSP nucleation. This alternate had been proposed by Witt (1969) and studied further by Sugiyama (1994); Goldberg and Witt measured mesospheric ionic content with a sounding rocket. Gumbel and Megner considered $H^+(H_2O)_n$ as the embryonic core nucleus, and this ionic process was deemed more favorable than nucleation on a neutral substrate because of the attraction of the dipole moment of a water molecule to the charge of a proton. The Gumbel and Megner model was based on CNT and proposed that the critical nucleus radius at which growth can overcome surface tension is ∼1 nm. The Gumbel and Megner model also proposed that the critical radius becomes zero for the case of ionic nucleation at sufficiently low temperatures. Although Gumbel and Megner suggested that the ionic scheme could surpass heterogeneous nucleation, they then dismissed the ionic scheme on the grounds that ambient electrons would quickly neutralize the proton hydrates so that this recombination would eliminate the advantages of a charged particle attracting water molecules. Gumbel and Megner proposed that negatively charged MSPs would instead provide a more plausible nucleus as these would not suffer recombination via electron collisions and yet would still exploit the attraction of water molecules to a charged nucleus. Hervig et al. (2012) interpreted optical properties of noctilucent clouds as indicating that ice grains contained small amounts of solid material that would be consistent with MSPs and so provide support for the negatively charged meteor smoke acting as nuclei. However, MSP remains a hypothetical concept as attempts to observe MSPs in an unambiguous way have so far failed (Hedin et al. 2014). As a further example that MSPs remain hypothetical, Stude et al. (2021) interpreted the negative ions observed by a rocket passing through the mesosphere as "likely due to negatively charged MSPs."

3. Nucleation from Negative Ions

The purpose of this paper is to argue that ice nucleation is indeed ionic as proposed by Gumbel and Megner but on negative ions rather than the positive ions considered by Gumbel and Megner. A negative ion would attract a water molecule just like a negatively charged smoke particle and, being negative, would similarly be immune to recombination via electron impact. The question then is whether the proposed negative ions exist.

There is substantial evidence for the existence of negative ions in various plasmas, but this evidence is generally indirect because direct observation of negative ions is difficult. The difficulty arises because negative ions have negligible spectroscopic footprint so their existence cannot be easily demonstrated by remote spectroscopic observation. Two types of indirect measurement have been used. The first is to make precise measurements of the electron and the positive ion densities. Because the plasma is expected to be quasi-neutral, if measurements indicate an electron density lower than the positive ion density, then there must be negative ions to provide the overall quasi-neutrality. The second method is to transiently detach electrons from the negative ions using energetic photons and then measure a transient increase in the electron density using probes or microwaves. The problem with indirect methods is that their interpretation is complex and requires numerous assumptions and models. Direct measurement would clearly be preferable. The most obvious direct measurement method is the direct collection of negative ions,

but this is impossible for astrophysical situations and difficult for laboratory situations. On the other hand, negative ions are routinely observed in the low-altitude atmosphere (troposphere). There is little observational information at mesospheric altitudes where any depletion of electrons relative to ions has generally been attributed to dust rather than ions capturing electrons. The possibility of negative ions in the mesosphere has been dismissed by Baumann (2016) on the grounds that atomic oxygen, which has significant density in the mesosphere, acts as a sink for negative ions; this conclusion was based on laboratory experiments by Fehsenfeld et al. (1966) investigating the $O + O^- \rightarrow O_2 + e$ reaction (the relevance and validity of this conclusion will be addressed in a later paragraph).

Below is a list of several relevant situations showing that plasmas can contain negative ions. These examples show that plasmas can contain negative ions of oxygen, hydrogen, hydroxyl, and sulfur hexafluoride.

Nguyen et al. (2009) measured electron and ion densities in an argon–water plasma and found that the free electron density was suppressed compared to that of a pure argon plasma. This was attributed to electrons attaching to atoms or molecules such as hydroxyl and oxygen.

Howling et al. (1994) observed growth of highly polymerized negative polysilicon hydride molecules in a silane (SiH_4) plasma and suggested that negative ions are the precursors to particle formation. Because electrons move faster than ions, electrons leave the bulk plasma faster, giving the bulk plasma a positive potential. This constitutes a potential well for negative ions and so negative ions have near-perfect confinement, which provides ample time for negative ions to interact with other species. The negative ions are presumed to induce a dipole moment in silane molecules so that there is then an attraction between the negative ion and the silane. This continues to attract other silane molecules so a large well-confined negative structure is developed. This process has been reviewed by Girshick (2020).

Using a Wien $E \times B$ filter, Renaud et al. (2015) observed negative fluorine atoms in a SF_6 discharge ion thruster.

Millar et al. (2017) reviewed negative ions in astrophysical environments and noted that the ratios of negative hydrogen atoms and negative hydrocarbon molecules (C_4H^-, C_6H^-, etc.) to neutrals can be as high as 10%.

Coates et al. (2010) detected negative ions in the plume of Enceladus and interpreted these as negative water clusters.

Arshadi & Kebarle (1970) observed gas-phase hydrates of OH^-, i.e., $OH^-(H_2O)_n$ in water vapor containing traces of hydrogen peroxide and in pure water. They also observed gas-phase hydrates of O_2^-, i.e., $O_2^-(H_2O)_n$. Kebarle et al. (1968) observed gas-phase hydration of F^-, Cl^-, Br^-, I^-, O_2^-, and NO_2^-. Meot-Ner (1986) also measured the production of $OH^-(H_2O)_n$. Newton & Ehrenson (1971) reported ab initio calculations of the formation of $OH^-(H_2O)_n$.

Sirse et al. (2017) observed O^-, F^-, and CF_3^- in an $Ar/O_2/C_4F_8$ capacitively coupled rf discharge using a diagnostic involving laser photoemission and resonance shift of a hair-pin probe.

Gregory et al. (2019) made ab initio molecular dynamics studies of the formation of $O_2^-(H_2O)_n$ and found very stable structures.

Witt (1969) considered ion hydrates forming noctilucent clouds and mainly considered positive ions although mentioned the possibility of a NO_2^- hydrate. Kopp (1992) reported rocket observations of several types of negative ions during a solar eclipse in 1979 at altitudes from 56.2 to 67.2 km. Stude et al. (2021) reported observations of many types of negative ions at locations inside a polar mesospheric winter echo layer.

Jungen et al. (1979) presented experimental data showing that electrons with energy exceeding approximately 4.5 eV would dissociate water to produce hydroxide (negative hydroxyl ion, i.e., OH^-); thus, tail electrons in an approximately 2 eV plasma could produce hydroxide.

Shimizu et al. (2010) observed using mass spectrometry an increase in DO (hydroxyl with deuterium) from the background level in their D_2–H_2 weakly ionized plasma when the electrodes were not cooled so no ice dust was formed. However, they saw a very slight decrease in DO if the electrodes were cooled so that ice dust was formed.

Fehsenfeld & Ferguson (1974) observed that, in the presence of water vapor, O^- would be depleted and replaced by OH^-, which would then form hydrates of the form $OH^-(H_2O)_n$. The measurement was done in an O_2 background which would be expected to contain atomic oxygen in association with the O^- production, but there apparently was no report of depletion of OH^- by atomic oxygen. This suggests that the conclusion by Baumann (2016) that all negative ions would be depleted by atomic oxygen does not occur in the presence of water vapor as the situation becomes more complicated than having only the $O + O^- \rightarrow O_2 + e$ reaction.

Peverall et al. (2020) observed O^- in the presence of a much larger atomic oxygen density in an O_2 discharge. The O^- density was as much as five times larger than the free electron density; this observation further counters the assertion by Baumann (2016) that negative ions cannot exist in the presence of atomic oxygen.

Based on the observations listed above, it is proposed here that, as observed by Fehsenfeld & Ferguson (1974), negative ions exist in a weakly ionized plasma containing some combination of water molecules, hydrogen molecules, and oxygen molecules. Because a water molecule has a very large dipole moment, it will be attracted to a region of strong electric field; this has been demonstrated by Libbrecht & Tanusheva (1999) and by Bartlett et al. (1963). Thus, there will be an attractive force between a neutral water molecule and a negative ion such as O_2^- or OH^-. The result of this attraction will be formation of a hydrate such as the $OH^-(H_2O)_n$ observed by Arshadi & Kebarle (1970) and by Fehsenfeld & Ferguson (1974). The number n of water molecules in the hydrate will increase with time because the hydrate will remain charged. Discharging would require a collision with a positive ion, but this will rarely happen because, relative to electrons, ions are very slow moving. If the temperature is low, the growing hydrate will become an ice grain rather than a liquid water drop. Thus, the critical ingredients are a cold, weakly ionized plasma containing molecules/atoms with large electron affinities so that some plasma electrons can attach to these species to form negative ions to which water molecules can attach and create negative ion hydrates. These ingredients exist in a weakly ionized plasma containing some combination of water molecules, hydrogen molecules, and oxygen molecules. It is thus highly likely that the rapid homogeneous nucleation observed in the Caltech water-ice experiment occurs in this sequence: formation of weakly ionized plasma (free electrons and ions in a sea of neutrals), dissociation of water into

Table 2
Electron Affinities of Atoms and Molecules Obtainable from Water

Species	Electron Affinity Energy E_a (eV)
O	1.43
O_2	0.45
H	0.76
OH	1.82

hydroxyl and hydrogen atoms, hydroxide formation, hydrate on hydroxide, growth of hydrate to macroscopic ice grain. Because of continuous electron and ion bombardment with electron flux exceeding ion flux, the ice grain will become increasingly negatively charged in the usual dusty plasma sense (Bellan 2020) as it becomes larger and so will continue to attract water molecules and grow.

An observed feature of the Caltech ice dusty plasma experiment is that the initiation of nucleation requires operation above a threshold pressure but once nucleation has begun, it proceeds faster and yields larger particles at pressures lower than this threshold; this feature is seen no matter what species of background gas is used. For example, Marshall et al. (2017) observed that the threshold for the nucleation of ice grains in an argon plasma containing a small amount of water vapor was 600 mT but, once nucleated, the ice grains would grow quickly at lower pressures. The main plasma parameters that change with neutral pressure are electron temperature and ion density. Bora et al. (2013) have shown that for a plasma with similar parameters the electron temperature decreases with increased pressure while the density has a nonmonotonic behavior, first increasing and then decreasing (see Figure 10 in Bora et al. 2013). The production of negative ions is likely strongly affected by electron temperature because the electron affinity is comparable to electron temperatures whereas the effect of electron density is expected to be less because, unlike electron affinity, there is no resonance-like condition.

A related observed feature of the Caltech ice dusty plasma is that nucleation does not occur if there is too much rf power. Specifically, Chai & Bellan (2015a) reported that rf power must not be higher than a certain value (0.5 W) but then once nucleation occurred, the rf power could be increased and then the ice grains would grow to a large size. Operation above a critical rf power likely corresponds to operating above a critical electron temperature, suggesting that nucleation is inhibited if the temperature of bulk electrons exceeds some critical value; Figure 6 in Bora et al. (2013) shows that the electron temperature increases with rf power.

This suggests that the bulk electron temperature should not be so high as to knock electrons off from negative ions. The most likely candidates for forming negative ions in a plasma containing water molecules are atomic hydrogen, atomic or molecular oxygen, and hydroxyl radicals; electron affinities E_a for these species are listed in Table 2.

Table 2 suggests that the most likely candidate for dominant negative ion in a water-containing capacitive discharge plasma is hydroxide (OH^-) as the electron temperature in such a plasma is $\sim$2 eV (Bora et al. 2013). Plasma electrons at 2 eV would thus have more than enough energy to knock electrons off from O_2 molecules or H atoms, but 2 eV electron energy would be marginal or insufficient for detaching bound electrons from O atoms or OH radicals. While O has an electron affinity similar to OH, as will be seen below, generation of O from water requires more energy than the generation of OH so the O path is less favorable. As support for the contention that OH^- is likely the predominant negative ion, it is noted that Nguyen et al. (2009) saw evidence of strong OH peaks in both the optical and mass spectra of a water plasma but only a small O_2 peak in the mass spectrum and an even smaller O peak. Sturm et al. (2010) observed simultaneous existence of H_2O, O, and OH in a protoplanetary disk so the necessary ingredients for forming negative ion hydrates exist in a protoplanetary disk, namely cold background gas, weak ionization, H_2O, O, and OH. It is thus expected based on the energy arguments from the lab plasma context that in a protoplanetary disk hydroxide would also be the most likely negative ion for forming hydrates.

Table 3
Electron Energy in eV at Which Negative Ions First Appears When Water Vapor Is Bombarded with Electrons, Electron Energy at which Negative Ion Yield has Peak, and Presumed Reaction

Ion	Appearance (eV)	Peak Production E_p (eV)	Formation Mechanism
H^-	4.8	6.0, 8.0 (weak)	$H_2O+e \rightarrow H^- + OH$
OH^-	4.7	6.1, 8.5, 11.2	$H^- + H_2O \rightarrow OH^- + H_2$
O^-	7.4	9.2, 11.2	$H_2O+e \rightarrow O^- + 2H$ (or H_2)

Note. Data are from Cottin and uncertainties in potential are typically $\pm$0.2 volts.

Cottin (1959) provided extensive measurements of how the production of positive and negative ions from electron bombardment of water vapor depends on the electron kinetic energy E. These measurements showed that ion production peaks at specific values of E; more recent data have been provided by Fedor et al. (2006). Table 3 lists Cottin's results for the lowest electron energy E that produces negative ions from water molecules and also the kinetic energies denoted as E_p at which this negative ion production is at a peak. The energies reported by Cottin for the production of positive ions by electron bombardment of water molecules are $\geqslant$12.6 V so in a plasma where $T_e \ll 12.6$ eV, negative ions should be the dominant type of ion produced by electron bombardment of water molecules.

Cottin (1959) observed that the production of OH^- was proportional to the square of the water vapor pressure whereas the production of H^- and O^- was linearly proportional and concluded from this observation that OH^- production is a two-step process where the first step is either

$$H_2O + e \rightarrow H^- + OH \quad (1)$$

or

$$H_2O + e \rightarrow O^- + 2H \text{ (or } H_2), \quad (2)$$

which would then be followed by a second step of either

$$H^- + H_2O \rightarrow OH^- + H_2 \quad (3)$$

or

$$O^- + H_2O \rightarrow OH^- + OH. \quad (4)$$

The need for two steps, each involving H_2O, would lead to the quadratic dependence on water vapor pressure. Fedor et al. (2006) observed a linear dependence of OH^- formation on water vapor pressure but the Fedor et al. measurements were made at a much lower water vapor pressure so the quadratic

path might have become insignificant relative to some linear single step path. Also, Fedor et al. noted theoretical arguments against a linear dependence. The path involving H^- in the second step (i.e., Equation (3)) seems more likely than the path involving O^- (i.e., Equation (4)) because, as listed in Table 3, the electron energy required to form O^- is substantially higher than that required to form H^-. Cottin's plot of OH^- production as a function of electron energy shows three maxima where the lowest of the three peaks (6 V) corresponds to a peak for the production of H^- and the highest of the three peaks (11.2 V) corresponds to a peak for the production of O^-.

It is proposed here that in order to produce negative hydrates in a weakly ionized plasma containing water vapor, a low T_e is desirable to avoid knocking electrons off from electronegative ions while a high T_e is desirable to create these electronegative ions. Because these requirements are conflicting, the optimum T_e should have a value intermediate between the affinity energy of a negative ion and the lowest electron energy peak for creating the negative ion. For hydroxide, the lowest electron energy peak is 6 eV. By expressing the electron Maxwell-Boltzmann distribution in terms of energy, the probability that an electron has a kinetic energy between E and $E+dE$ is

$$f(E)dE = 2\sqrt{\frac{E}{\pi}}\frac{1}{(T_e)^{3/2}}\exp\left(-\frac{E}{T_e}\right)dE, \tag{5}$$

where the electron kinetic energy E and the electron temperature T_e are both measured in electron volts. Electrons that have kinetic energy E exceeding the affinity energy E_a of an electron attached to a negative ion will detach the bound electron, in a manner similar to an energetic electron ionizing a neutral atom or molecule. This is analogous to laser photodetachment (Sirse et al. 2017), where a photon with energy exceeding E_a detaches the bound electron from a negative ion. The flux F_d of "detaching" electrons having $E > E_a$ is

$$\begin{aligned} F_d &= n_e\int_{E_a}^{\infty}\left(\frac{2E}{m_e}\right)^{1/2} f(E) \\ dE &= n_e\left(\frac{8T_e}{\pi m}\right)^{1/2}\left(\frac{E_a}{T_e}+1\right)\exp\left(-\frac{E_a}{T_e}\right). \end{aligned} \tag{6}$$

The flux of attaching electrons, i.e., electrons having energy at the energy E_p as listed in the third column of Table 3, is found by multiplying Equation (5) by the electron velocity $v \propto \sqrt{E_p}$ and density n_e to obtain

$$F_a = \lambda n_e\frac{E_p}{(T_e)^{3/2}}\exp\left(-\frac{E_p}{T_e}\right), \tag{7}$$

where λ is a coefficient proportional to the width of the peak.

Thus, F_a characterizes the rate at which negative ions are created while F_d describes the rate at which they are destroyed. The ratio of these two fluxes consequently gives a rough figure of merit for the value of T_e that maximizes creation of negative ions. This ratio is

$$\frac{F_a}{F_d} = \mu\frac{E_p}{(T_e)^2}\frac{\exp\left(\frac{E_a-E_p}{T_e}\right)}{\left(\frac{E_a}{T_e}+1\right)}, \tag{8}$$

where μ is a constant incorporating the factors that do not involve T_e.

Figure 1 plots F_a/F_d for the hydroxide situation, where $E_a = 1.82$ eV and $E_p = 6$ eV. This plot peaks at $T_e = 2.65$ eV, which is of the order of the T_e presumed for the Caltech ice dusty plasma. This ratio F_a/F_d is a rough figure of merit because it does not account for additional issues such as the stronger detachment of bound electrons by incident electrons with $E \gg E_a$ compared to those with $E \gtrsim E_a$ and the possibility of a non-Maxwellian two-temperature electron velocity distribution such as reported by Godyak & Piejak (1990). The peak in Figure 1 at a low but finite electron temperature is consistent with the observation that nucleation in a weakly ionized plasma occurs at low rf power (Chai & Bellan 2015a) and at high background gas pressure (Marshall et al. 2017), because both of these regimes imply low T_e. Shimizu et al. (2010) observed (Figure 5 in their paper) an increase of DO upon formation of a weakly ionized deuterium-oxygen plasma when the electrodes were not cooled (no ice nucleation, Figure 5(b)) but a slight decrease of DO when the electrodes were cooled (ice dust nucleation seen, Figure 5(a)). This observation is consistent with DO being absorbed into negative ion hydrates $DO^-(D_2O)_n$ as the initial step in homogeneous ice nucleation in a weakly ionized cold plasma containing D_2O molecules. Shimuzu et al.'s observation in their Figure 5(c) that DO increased when the cooling was removed is consistent with DO no longer being absorbed when ice nucleation stops. This is circumstantial evidence because a conventional mass spectrometer does not observe negative ions because its internal acceleration is arranged for positive ions. Shimizu et al. were thus likely measuring neutral DO but this could be considered a proxy for DO^-.

4. Critique of CNT

The plausibility of this negative ion nucleation hypothesis is bolstered by noting that certain aspects of CNT involve using a theory outside its range of validity. CNT is based on thermodynamics but the essential assumption underlying thermodynamics is inappropriate for a dusty plasma because the electrons are much hotter than the ions and neutrals (e.g., electron temperature is of the order of 10^4 K whereas ions and neutral temperature are of the order of 10–10^2 K). The essential assumption of thermodynamics, namely that all constituents are at the same temperature, is thus clearly violated. The Gibbs free energy, an important quantity in CNT, is undefined in a weakly ionized plasma because Gibbs free energy is defined for fixed pressure and fixed temperature. Because a weakly ionized plasma cannot be characterized by a single temperature, the Gibbs free energy is not meaningful in a weakly ionized plasma.

A related aspect that casts doubt on CNT is that application of CNT to ice nucleation presumes that the surface tension of liquid water can be extrapolated to apply to ice, but extrapolating surface tension from liquid to solid is debatable as noted by Makkonen (2012), who showed that solids do not have surface tension in the same sense as liquids. The surface of ice in terrestrial conditions is known to be coated by a quasi-liquid layer (QLL) that is a few molecules thick. At first sight, it seems that a QLL could conceivably provide a form of surface tension and so provide a basis for CNT. However, Slater & Michaelides (2019) showed that the QLL vanishes at temperatures <240 K so ice nucleation models for ordinary

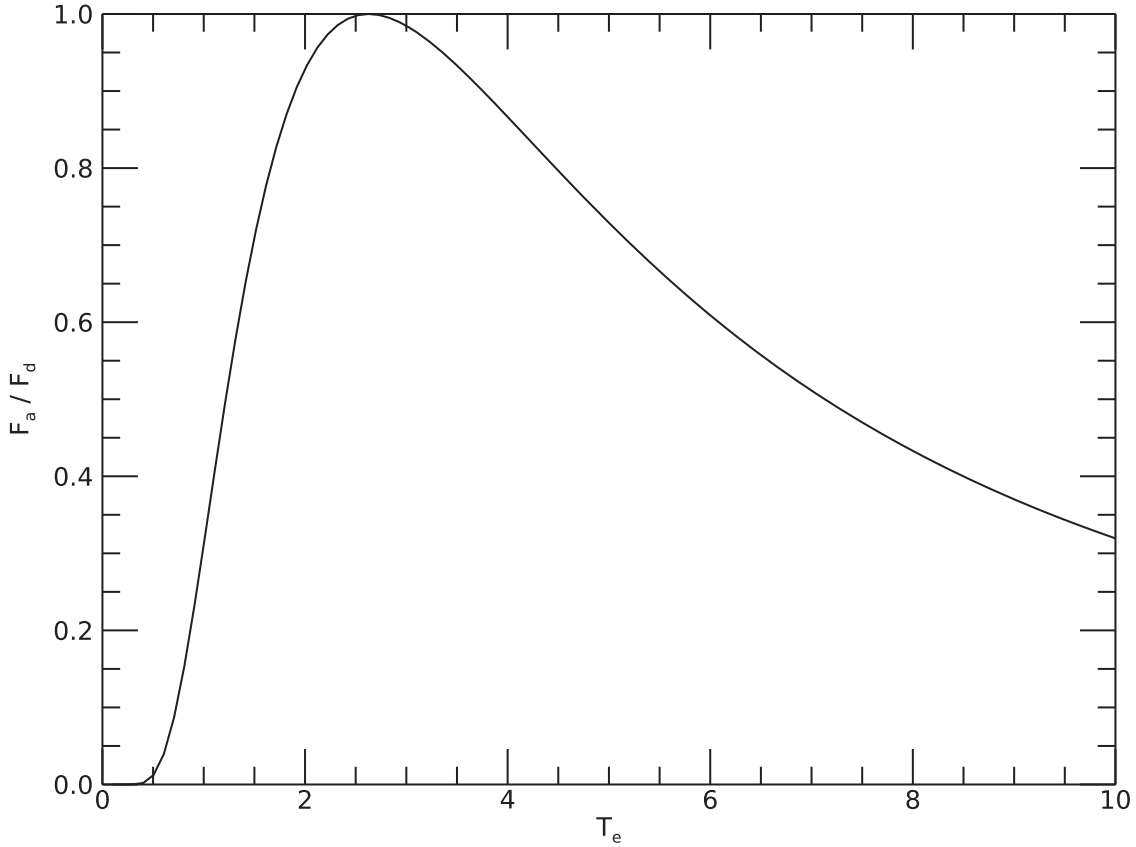

Figure 1. Plot of F_a/F_d normalized to its maximum value vs. T_e for hydroxide formation using electron affinity energy $E_a = 1.82$ eV and peak electron energy (Cottin 1959) for formation $E_p = 6$ eV.

terrestrial conditions (i.e., temperature exceeding 240 K) are inapplicable to the much colder astrophysical regime (i.e., $T \ll 240$ K). Concern about invoking surface tension in CNT even for liquid drops was noted by Tolman (1949) who stated, "as we consider smaller and smaller droplets of liquid phase, however, the concept of surface tension and the previously satisfactory thermodynamic methods seem less and less appropriate. Indeed, it will ultimately seem more satisfactory to continue the investigation using the concept of forces exerted by individual molecules and the more detailed methods of molecular mechanics." Homogeneous nucleation must begin by having two molecules bind together, but at this stage no surface exists so thermodynamic arguments involving surface tension are inappropriate. Thermodynamics implicitly presumes the presence of a large number of molecules, not two.

It should be noted that Murray & Jensen (2010) have previously advocated the possibility of homogeneous nucleation in the mesosphere, but the mechanism they proposed involved neutral water molecules rather than the negative ions proposed here. The negative ion mechanism should be more important because it results in a stronger bond. The first step in homogeneous nucleation involves two molecules sticking together. The effectiveness of the homogeneous water–water process proposed by Murray & Jensen (2010) can thus be compared to the hydroxide hydrate process proposed here by comparing how strongly the initial reacting two molecules stick together. This is done by comparing the respective enthalpy heats of reaction ΔH_r^0 of the Murray–Jensen mechanism and of the hydroxide hydrate mechanism proposed here. The Murray–Jensen homogeneous nucleation has the reaction

$$H_2O + H_2O \rightarrow (H_2O)_2;\ \Delta H_r^0 = -9\ \text{kJ mole}^{-1}, \quad (9)$$

whereas the process proposed here has the reaction

$$OH^- + H_2O \rightarrow OH^-(H_2O);\ \Delta H_r^0 = -115\ \text{kJ mole}^{-1}. \quad (10)$$

The reaction enthalpies are calculated using the Argonne National Lab Active Thermochemical Tables (Ruscic 2021). The hydroxide–water reaction has a much more negative enthalpy heat of reaction which indicates that $OH^-(H_2O)$ is a more stable state than two attached water molecules and so should be more important. This is in accord with the observation by Fehsenfeld & Ferguson (1974) that strong bonding occurs when OH^- associates with H_2O.

Stability of hydroxide hydride with respect to destruction by atomic oxygen can be checked by considering

$$O + 2[(OH-)(H_2O)] \rightarrow 3H_2O + O_2 + 2e, \quad (11)$$

where the stoichiometry has been arranged so the products are standard states, in which case no further spontaneous reactions should occur (water does not burn). The reaction enthalpy here is $\Delta H_r^0 = +9.4$ kJ mole^{-1}; thus, this reaction is endothermic and would not occur spontaneously (see the discussion in Fehsenfeld et al. 1966 where it was noted that reactions with $\Delta H_r^0 > 0$ were not observed). This means that hydroxide hydride is a stable state and will not be destroyed by interaction with atomic oxygen. This is in contrast to the reaction

$$O + O^- \rightarrow O_2 + e, \quad (12)$$

which has a reaction enthalpy $\Delta H_r^0 = -357$ kJ mole^{-1} and so is spontaneous, implying that oxygen anion will not endure in the presence of atomic oxygen unless oxygen anion is being continuously replenished.

In summary, the standard presumption that heterogeneous nucleation dominates homogeneous nucleation does not apply to the situation of a weakly ionized plasma consisting of a cold background gas with negative atoms or molecules. Because OH and H_2O commonly exist in various astrophysical situations, in the mesosphere, and exist in the ice dust lab experiments (Shimizu et al. 2010; Chai & Bellan 2015b), and because OH has a large electron affinity, homogeneous nucleation of ice via hydrates based on OH^- is likely to be operative in these situations. The OH^- density does not have to be large because each OH^- ion forms the nucleus for an ice grain that would have many attached electrons. The required OH^- density is thus so low that it would be difficult to prove that the OH^- density is inadequate.

The semiquantitative arguments presented here provide guidance for future, more precise analysis and measurements to determine which negative ion is indeed dominant and how the process scales to different parameter regimes. Motivated by these arguments, a diagnostic extending the methods used in Howling et al. (1994) to a water-ice dusty plasma is being constructed. This diagnostic will search for the negative ions predicted to exist as a precursor to the homogeneous nucleation of water ice and will determine how the negative ions depend on plasma parameters such as ion density, electron temperature, and background gas species and whether negative ion formation is the initial step to ice grain nucleation in a cold weakly ionized plasma containing water vapor.

Supported by the NSF/DOE Partnership in Basic Plasma Science and Engineering via USDOE Award DE-SC0020079.

ORCID iDs

Paul M. Bellan https://orcid.org/0000-0002-0886-8782

References

Arshadi, M., & Kebarle, P. 1970, JPhCh, 74, 1483
Bartlett, J. T., Heuval, A. P., & Mason, B. J. 1963, Zeitschrift fur angewandte Mathematik und Physik ZAMP, 14, 599
Baumann, C. 2016, PhD Thesis, Ludwig Maximilians Univ.
Bellan, P. M. 2020, ApJ, 905, 96
Bora, B., Bhuyan, H., Favre, M., et al. 2013, CAP, 13, 1448
Chai, K.-B., & Bellan, P. M. 2013, GeoRL, 40, 6258
Chai, K.-B., & Bellan, P. M. 2015a, JASTP, 127, 83
Chai, K.-B., & Bellan, P. M. 2015b, ApJ, 802, 112
Coates, A., Jones, G., Lewis, G., et al. 2010, Icar, 206, 618
Cottin, M. 1959, JCP, 56, 1024
Dong, Y., Hill, T. W., & Ye, S.-Y. 2015, JGRA, 120, 915
Fedor, J., Cicman, P., Coupier, B., et al. 2006, JPhB, 39, 3935
Fehsenfeld, F. C., & Ferguson, E. E. 1974, JChPh, 61, 3181
Fehsenfeld, F. C., Ferguson, E. E., & Schmeltekopf, A. L. 1966, JChPh, 45, 1844
Girshick, S. L. 2020, JVST, 38, 011001
Godyak, V. A., & Piejak, R. B. 1990, PhRvL, 65, 996
Gregory, N., Reveles, J. U., Bly, J., & Luong, T. 2019, JPCA, 123, 7528
Gumbel, J., & Megner, L. 2009, JASTP, 71, 1225
Hedin, J., Giovane, F., Waldemarsson, T., et al. 2014, JASTP, 118, 127
Hervig, M. E., Deaver, L. E., Bardeen, C. G., et al. 2012, JASTP, 84, 1
Howling, A. A., Sansonnens, L., Dorier, J.-L., & Hollenstein, C. 1994, JAP, 75, 1340
Hsu, H.-W., Schmidt, J., Kempf, S., et al. 2018, Sci., 362, eaat3185
Jones, A. P., & Williams, D. A. 1984, MNRAS, 209, 955
Jungen, M., Vogt, J., & Staemmler, V. 1979, CP, 37, 49
Kebarle, P., Arshadi, M., & Scarborough, J. 1968, JChPh, 49, 817
Kopp, E. 1992, AdSpR, 12, 325
Libbrecht, K. G., & Tanusheva, V. M. 1999, PhRvE, 59, 3253
Makkonen, L. 2012, Scripta Materialia, 66, 627
Marshall, R. S., Chai, K.-B., & Bellan, P. M. 2017, ApJ, 837, 56
Meot-Ner, M., & Speller, C. V. 1986, JPhCh, 90, 6616
Millar, T. J., Walsh, C., & Field, T. A. 2017, ChRv, 117, 1765
Moultaka, J., Eckart, A., & Muzic, K. 2015, ApJ, 806, 202
Murray, B. J., & Jensen, E. J. 2010, JASTP, 72, 51
Newton, M. D., & Ehrenson, S. 1971, JAChS, 93, 4971
Nguyen, S. V. T., Foster, J. E., & Gallimore, A. D. 2009, RScI, 80, 083503
Peverall, R., Rogers, S. D. A., & Ritchie, G. A. D. 2020, PSST, 29, 045004
Potapov, A., Bouwman, J., Jäger, C., & Henning, T. 2021, NatAs, 5, 78
Protopapa, S., Sunshine, J. M., Feaga, L. M., et al. 2014, Icar, 238, 191
Pruppacher, H., & Klett, J. 2010, Atmospheric and Oceanographic Sciences Library, Vol. 18, Microphysics of Clouds and Precipitation (Dordrecht: Springer Netherlands),
Rapp, M., Gumbel, J., & Lübken, F.-J. 2001, AnGeo, 19, 571
Rapp, M., & Thomas, G. E. 2006, JASTP, 68, 715
Renaud, D., Gerst, D., Mazouffre, S., & Aanesland, A. 2015, RScI, 86, 123507
Ruscic, B., & Bross, D. H. 2021, Active Thermochemical Tables (ATcT) values based on ver. 1.122r of the Thermochemical Network https://atct.anl.gov/Thermochemical%20Data/version%201.122r/index.php
Seki, J., & Hasegawa, H. 1983, Ap&SS, 94, 177
Shimizu, S., Klumov, B., Shimizu, T., et al. 2010, JGRD, 115, D18205
Sirse, N., Tsutsumi, T., Sekine, M., Hori, M., & Ellingboe, A. R. 2017, JPhD, 50, 335205
Slater, B., & Michaelides, A. 2019, Nat. Rev. Chem., 3, 172
Spilker, L., Ferrari, C., Cuzzi, J., et al. 2003, P&SS, 51, 929
Stude, J., Aufmhoff, H., Schlager, H., et al. 2021, AMT, 14, 983
Sturm, B., Bouwman, J., Henning, T., et al. 2010, A&A, 518, L129
Sugiyama, T. 1994, JGR, 99, 3915
Terada, H., Tokunaga, A. T., Kobayashi, N., et al. 2007, ApJ, 667, 303
Tolman, R. C. 1949, JChPh, 17, 337
Vahidinia, S., Cuzzi, J. N., Hedman, M., et al. 2011, Icar, 215, 682
Vaste, O. 1993, JATP, 55, 133
Witt, G. 1969, in COSPAR, Space Research IX, Proc. Tokyo 1968 (Amsterdam: North-Holland), 157
Woitke, P., Kamp, I., & Thi, W.-F. 2009, A&A, 501, 383
Zasetsky, A. Y., Petelina, S. V., & Svishchev, I. M. 2009, ACP, 9, 965